

Electronic Supplementary Material (ESI) for Journal of Materials Chemistry C.
This journal is © The Royal Society of Chemistry 2021

Supporting Information

Fluorescent Recognition of Adenosine Triphosphate and Uric Acid by two Eu-Based Metal-Organic Frameworks

Li-Juan Han,^{a, b,*} Ya-Jie Kong,^a Xing-Min Zhang,^a Guo-Zheng Hou,^a Hua-Chong
Chen,^a and He-Gen Zheng^{b, *}

^a *Department of Chemistry and Chemical Engineering, Jining University, Qufu, 273155, P. R. China*

^b *State Key Laboratory of Coordination Chemistry, School of Chemistry and Chemical Engineering, Collaborative Innovation Center of Advanced Microstructures, Nanjing University, Nanjing 210023, P. R. China*

* Corresponding authors: hanlij78@163.com; zhenghg@nju.edu.cn

Materials and instrumentation

All reagents and solvents were commercially available and used as received without further purification. The IR absorption spectra of these complexes were recorded in the range of 400-4000 cm^{-1} by means of a Nicolet (Impact 410) spectrometer with KBr pellets. Element analyses (C, H, N) were carried out on a Perkin-Elmer model 240C analyzer. PXRD measurements were performed on a Bruker D8 Advance X-ray diffractometer using $\text{Cu-K}\alpha$ radiation (0.15418 nm), in which the X-ray tube was operated at 40 kV and 30 mA. TG analysis was performed on a Perkin Elmer thermogravimetric analyzer from room temperature to 1000 $^{\circ}\text{C}$ with a heating rate of 10 $\text{K}\cdot\text{min}^{-1}$ under N_2 atmosphere. Photoluminescence spectra were recorded with a PerkinElmer FS-LS55 fluorescence spectrophotometer at room temperature.

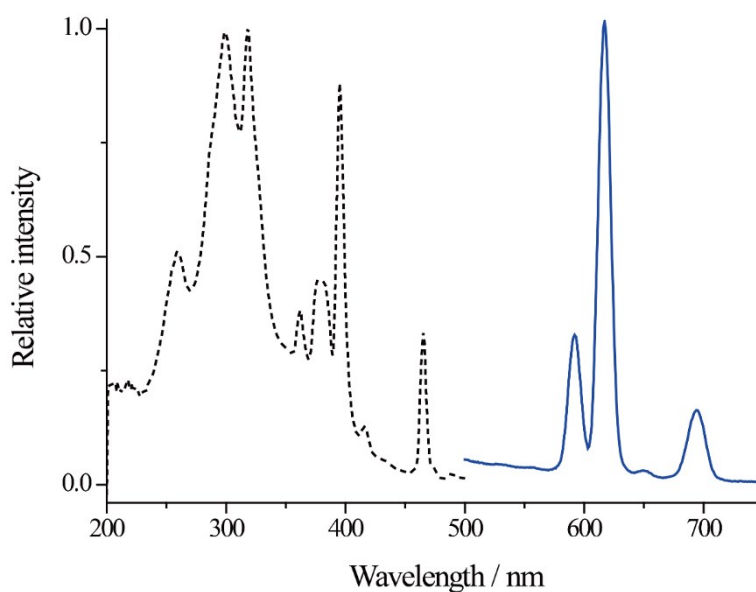


Fig. S1 Solid-state excitation (dotted black, $\lambda_{\text{em}} = 617 \text{ nm}$) and emission (solid blue, $\lambda_{\text{ex}} = 265 \text{ nm}$) spectra of compound **1**.

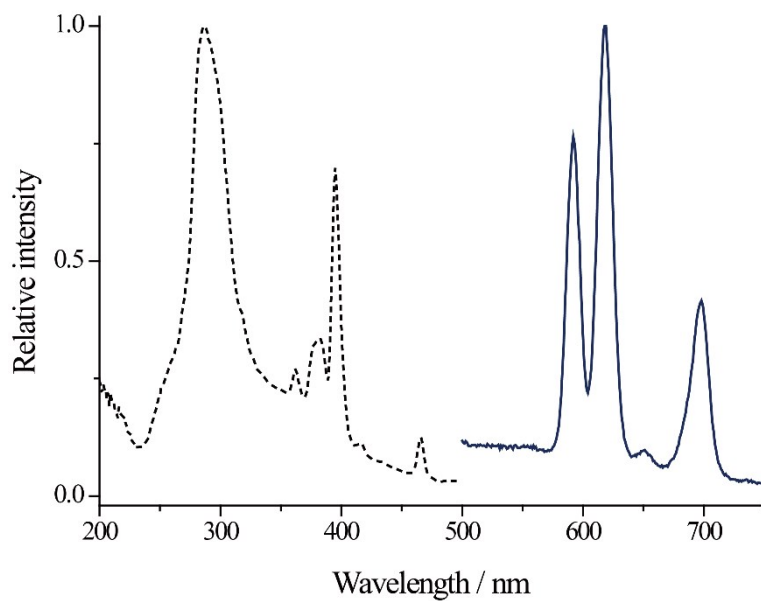


Fig. S2 Solid-state excitation (dotted black, $\lambda_{em} = 617$ nm) and emission (solid blue, $\lambda_{ex} = 265$ nm) spectra of compound **2**.

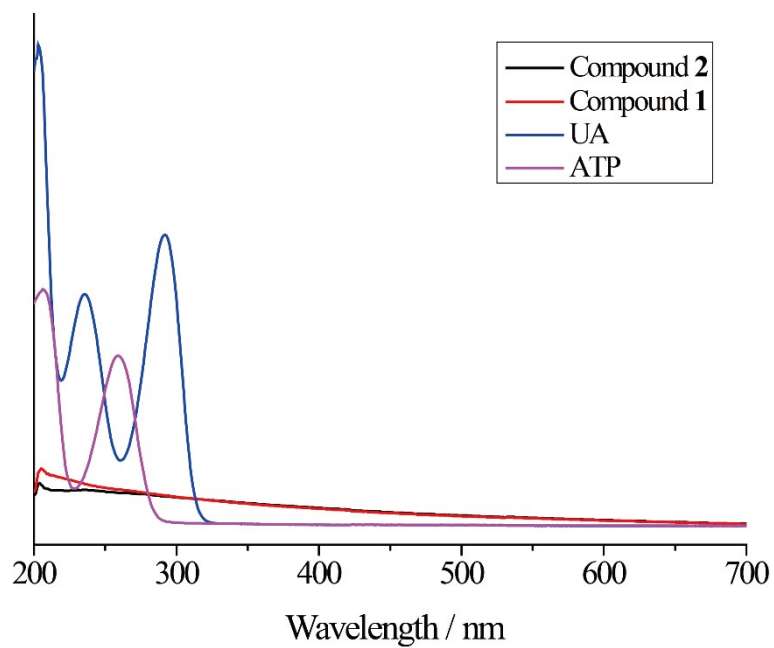


Fig. S3 Liquid UV-vis spectra of compound **1**, compound **2**, ATP and UA.

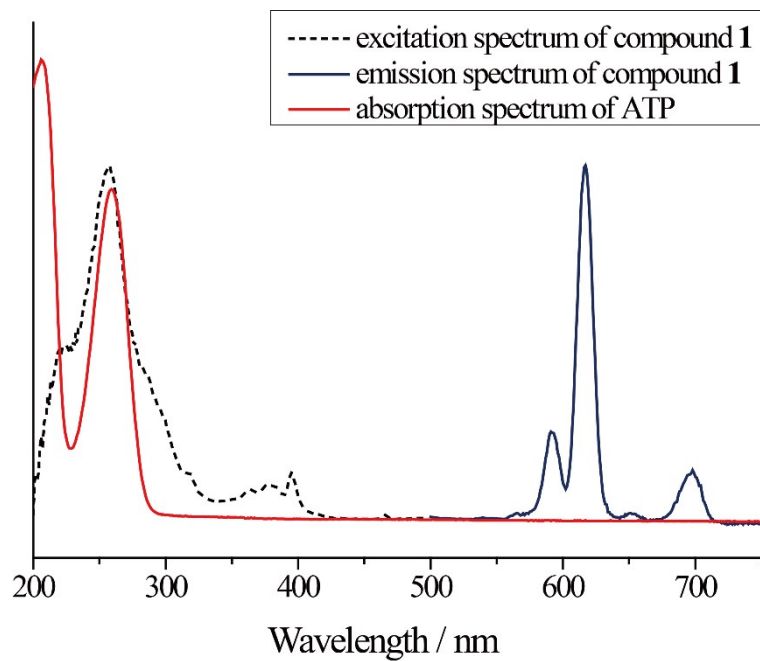


Fig. S4 Spectral overlap between the absorption spectra of ATP and the emission as well as excitation spectra of compound **1**.

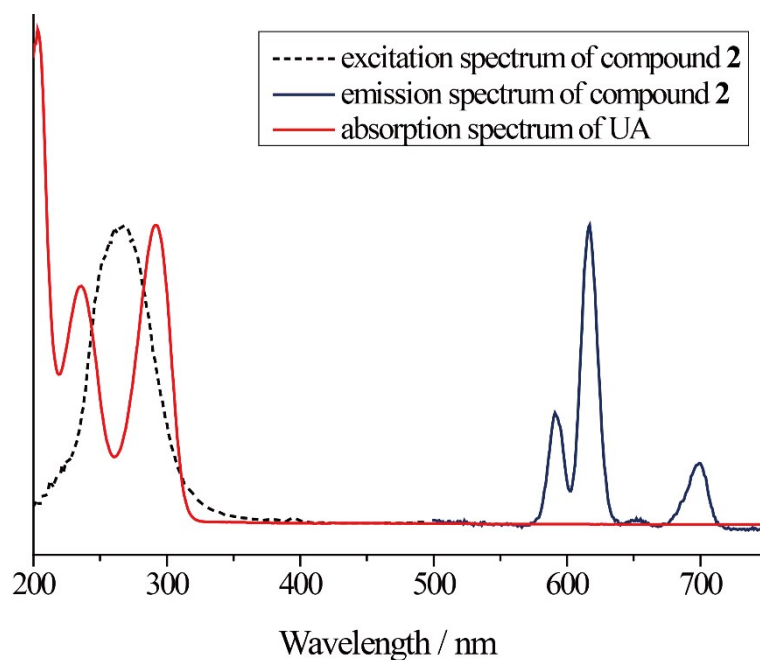


Fig. S5 Spectral overlap between the absorption spectra of UA and the emission as well as excitation spectra of compound **2**.

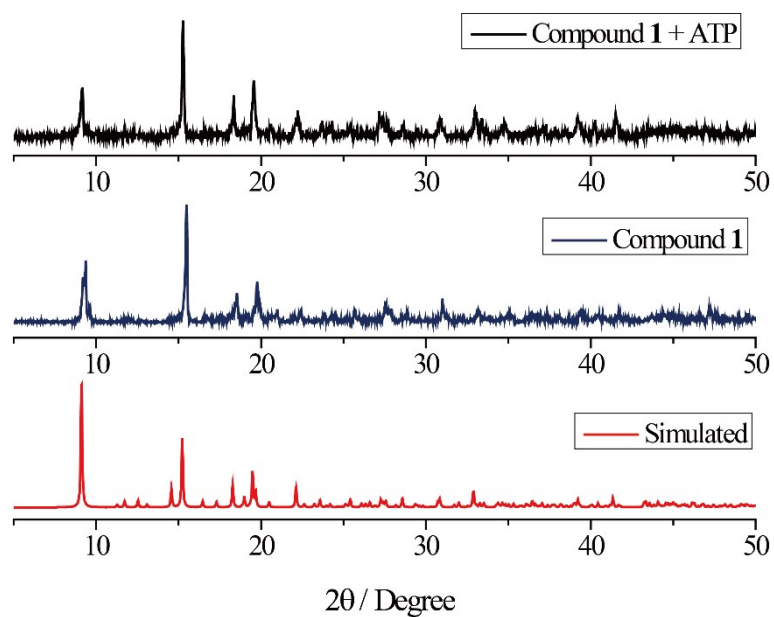


Fig. S6 PXRD of compound 1 before and after immersed in ATP 80 hours.

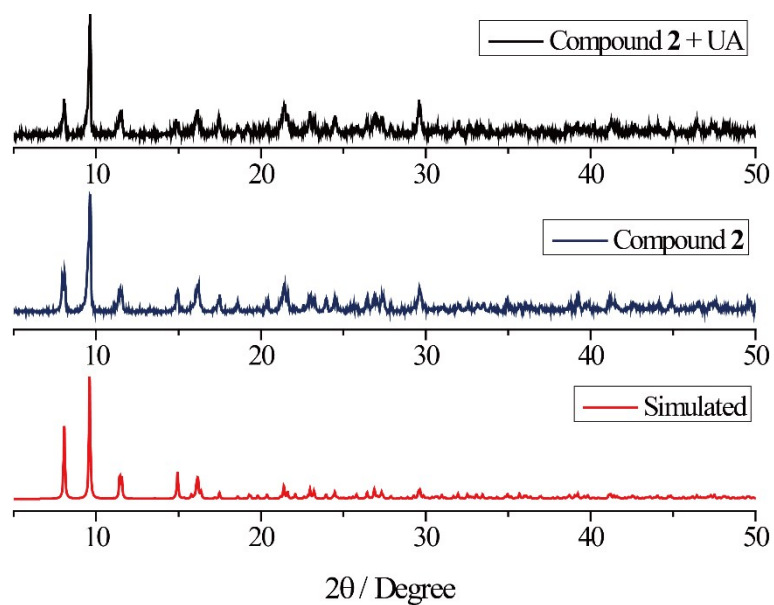
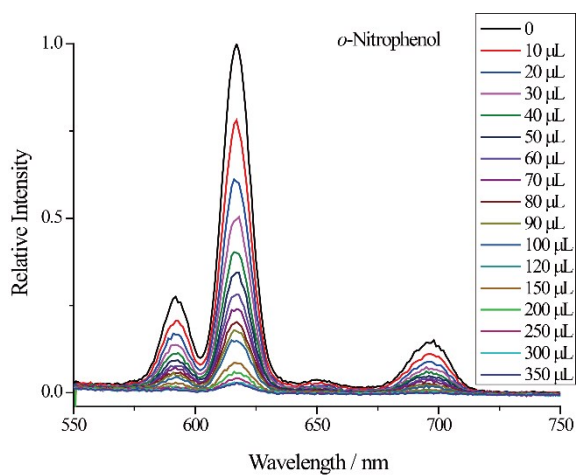
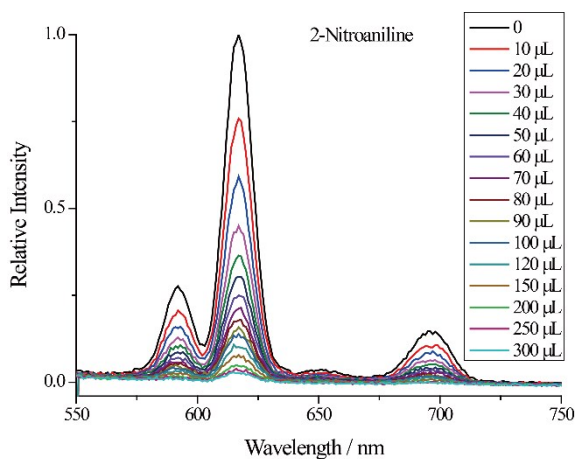
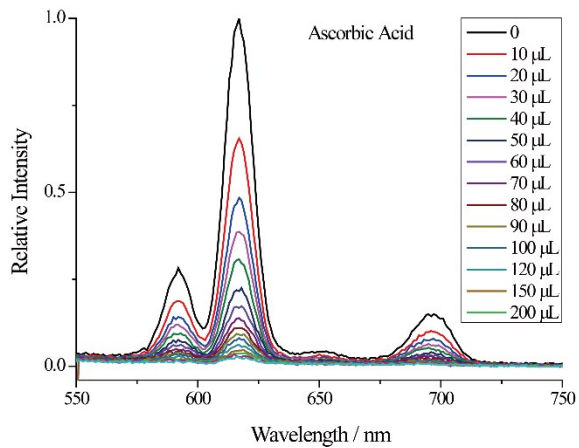
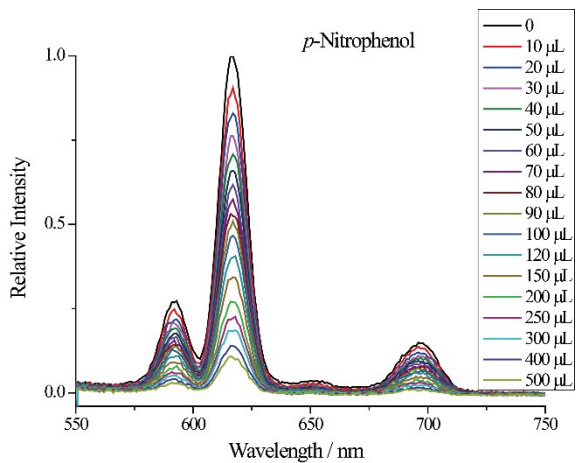
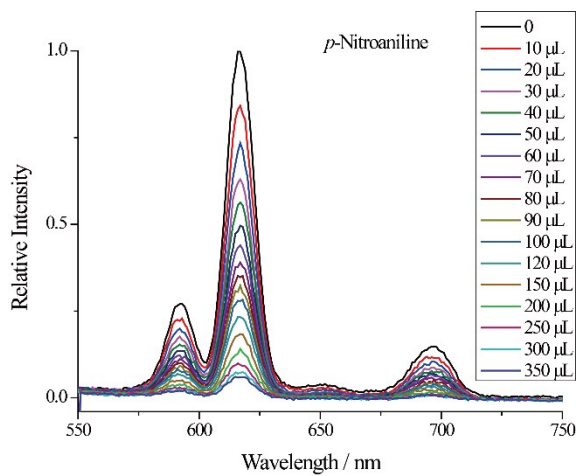
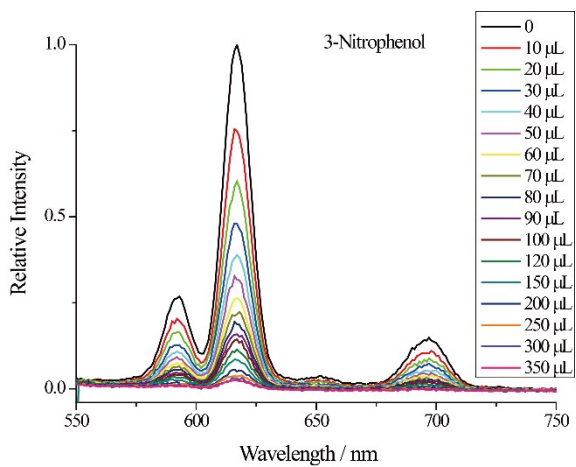


Fig. S7 PXRD of compound 2 before and after immersed in UA 80 hours.



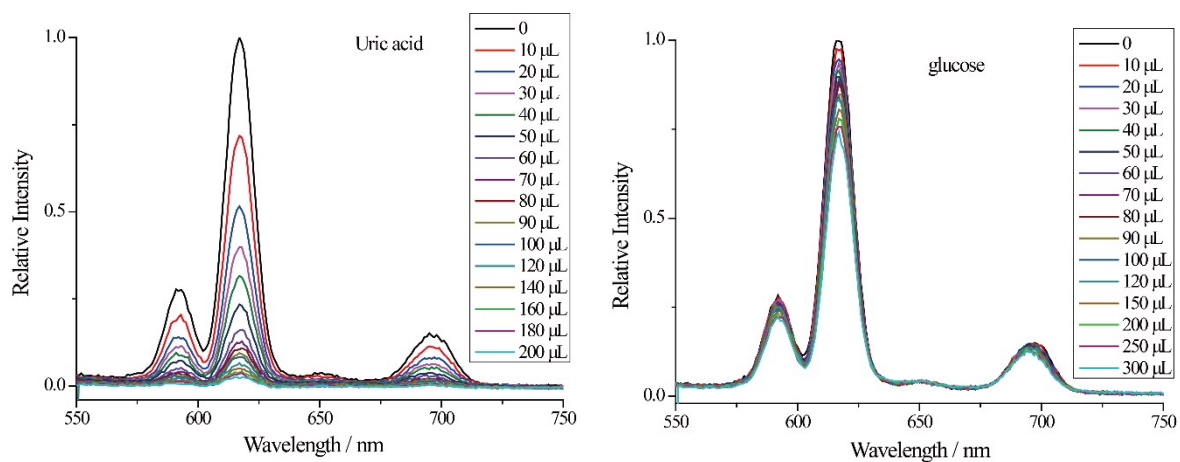
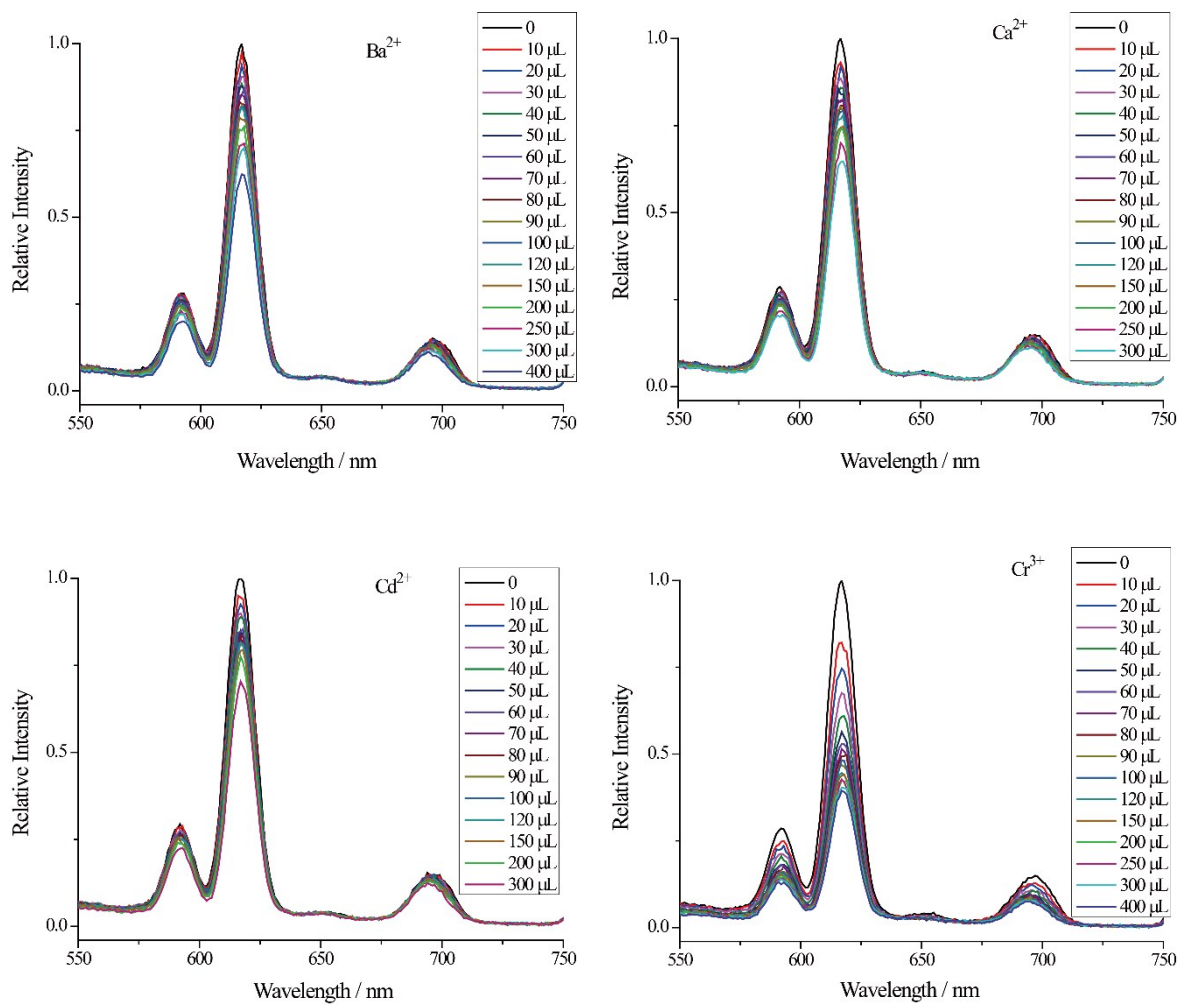
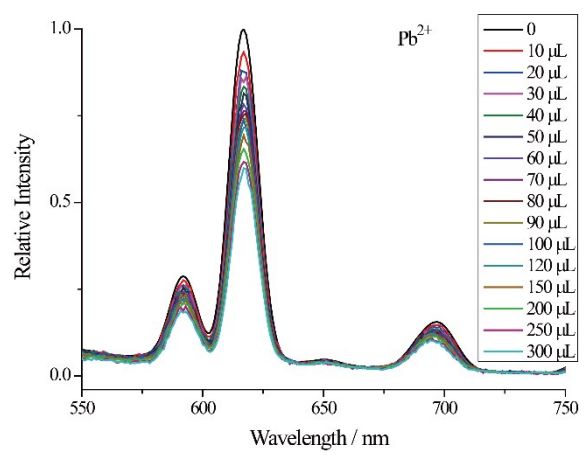
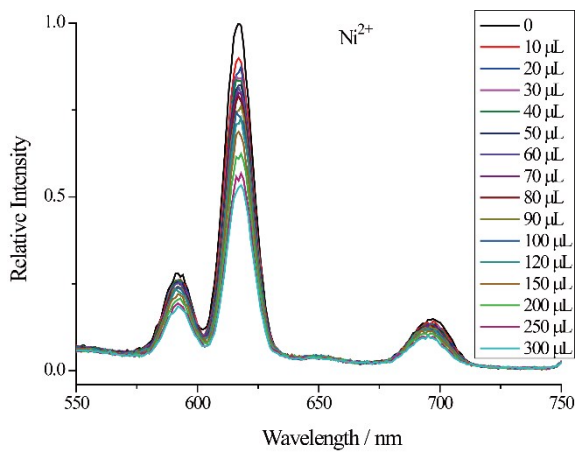
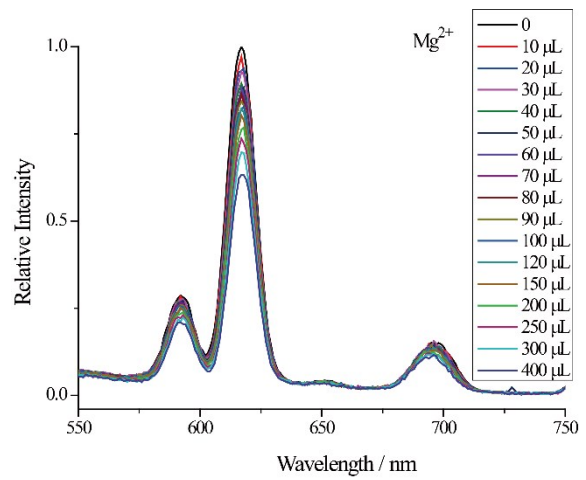
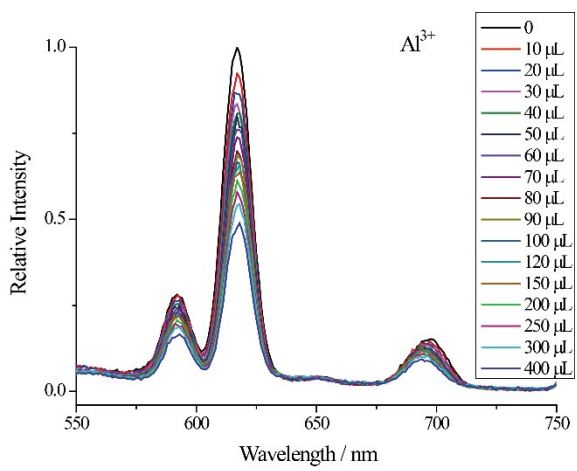
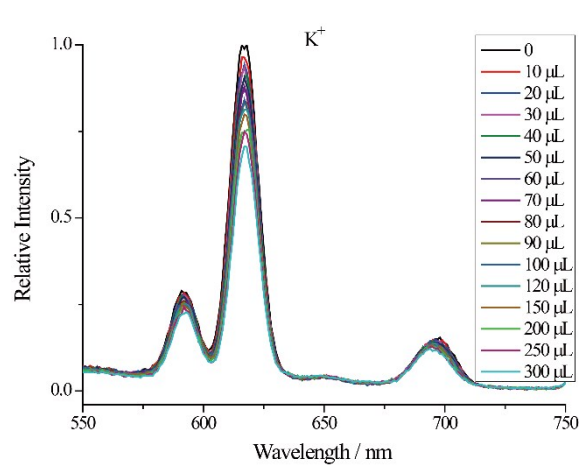
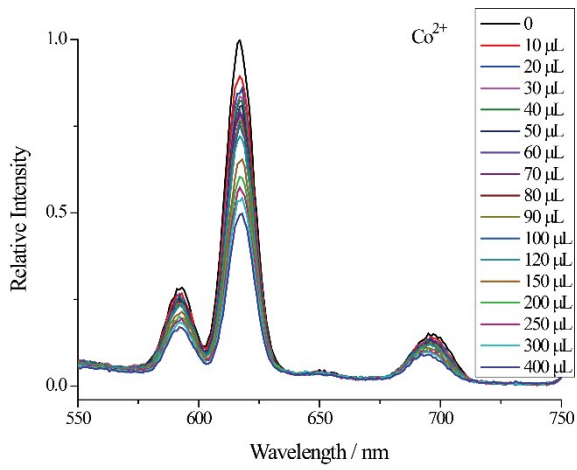


Fig. S8 Fluorescence spectra of compound **1** (ethanol suspension, 1.0 mL) before and after added various analytes (excited at 265 nm).





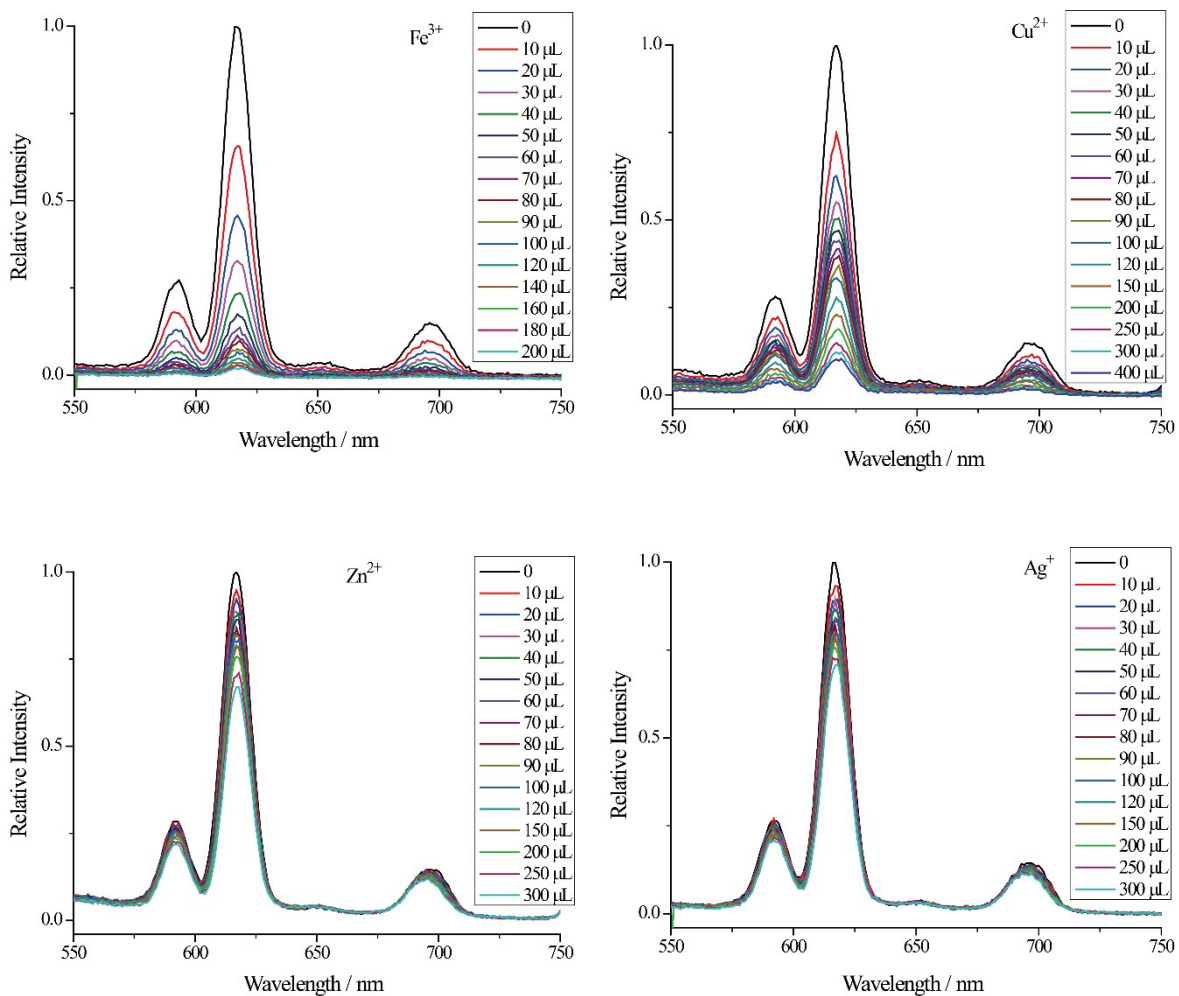
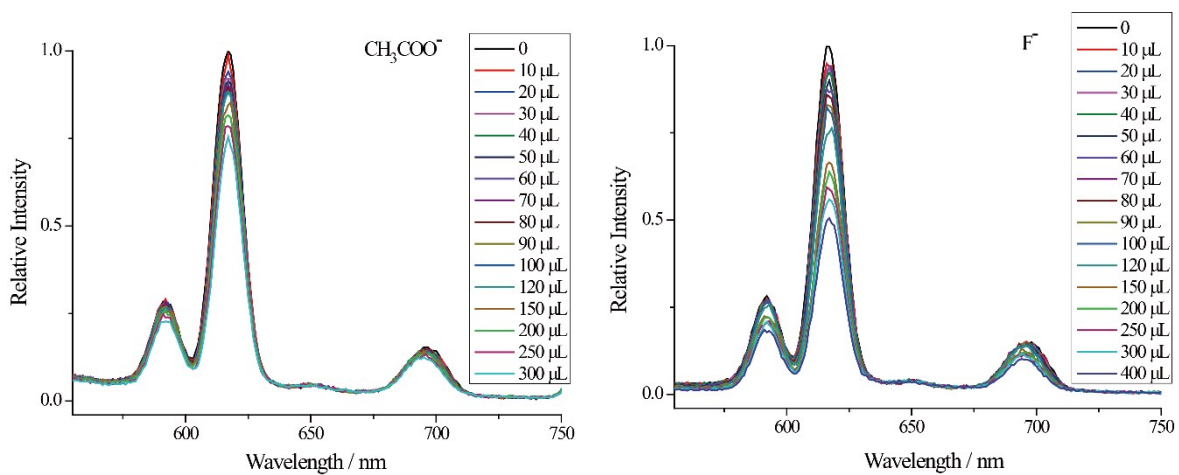
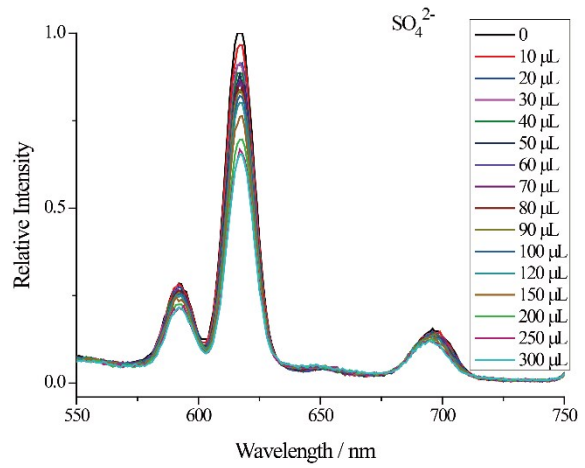
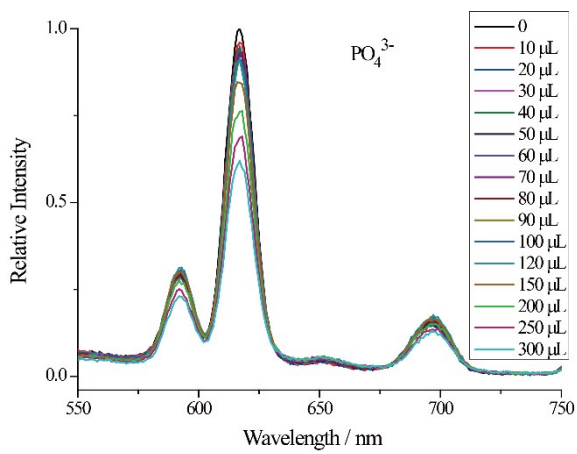
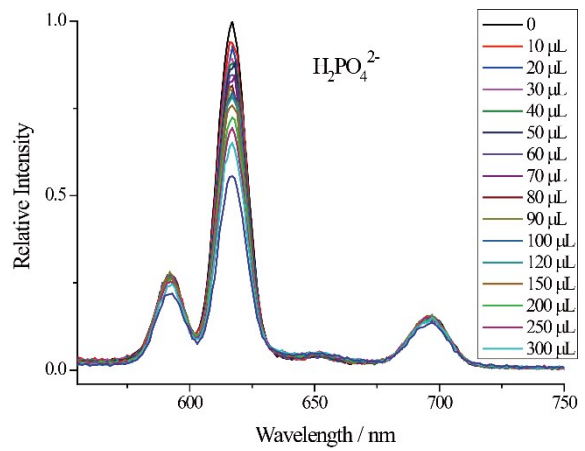
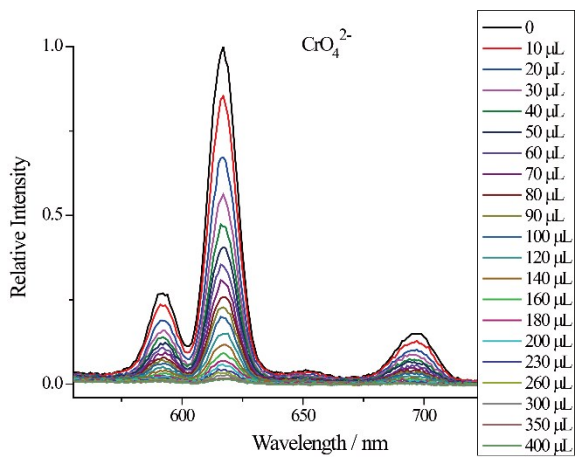
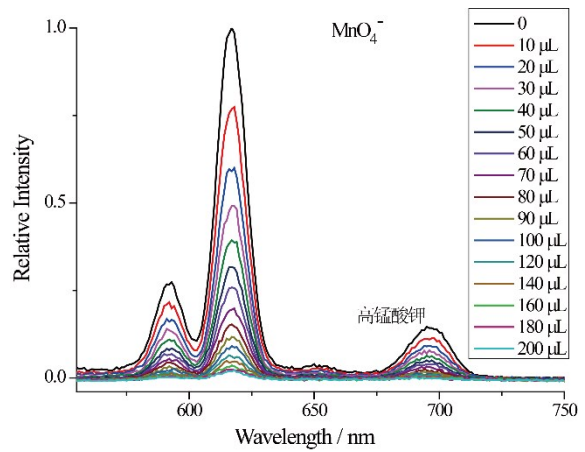
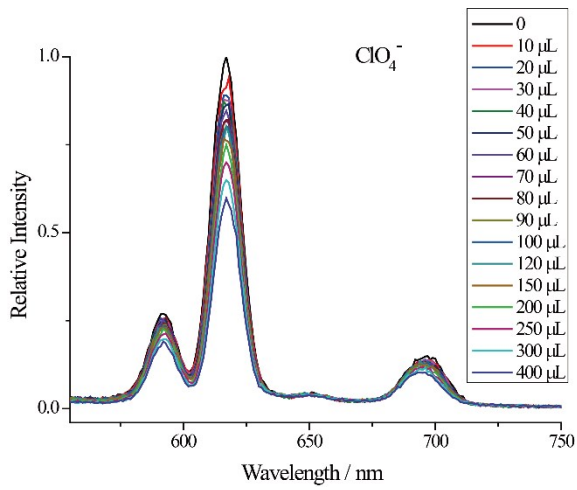


Fig. S9 Fluorescence spectra of compound **1** (ethanol suspension, 1.0 mL) before and after added different metal ions (excited at 265 nm).





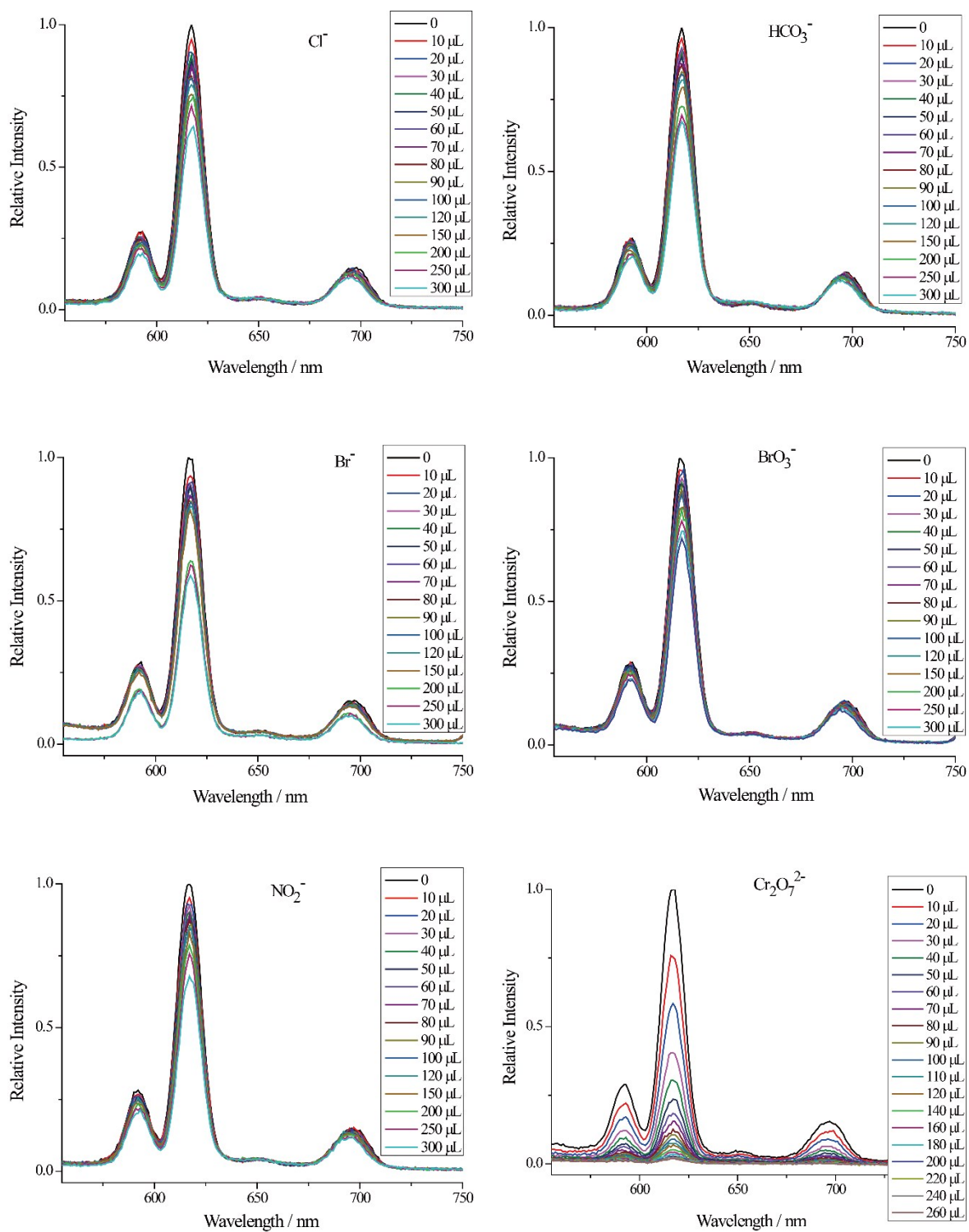
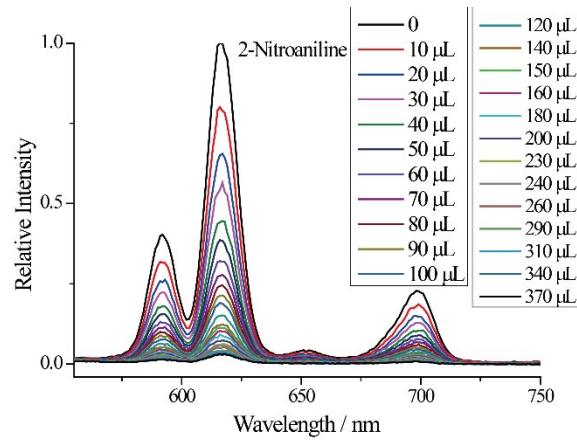
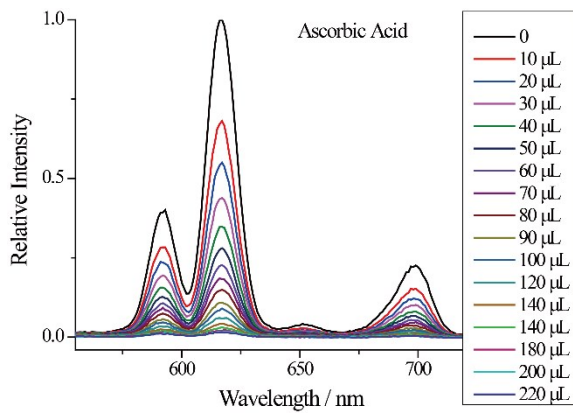
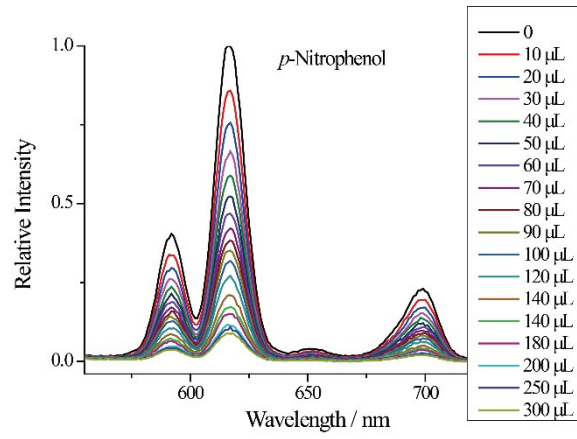
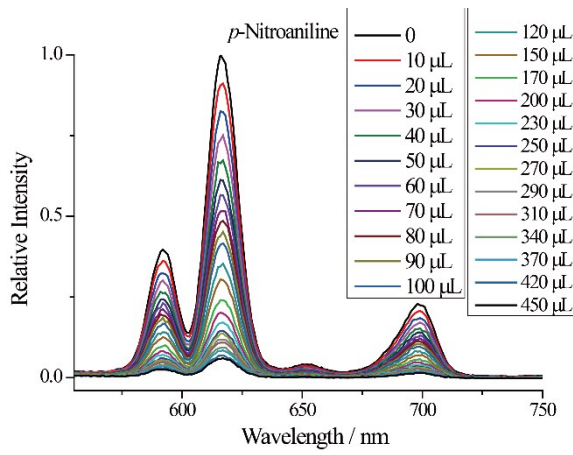
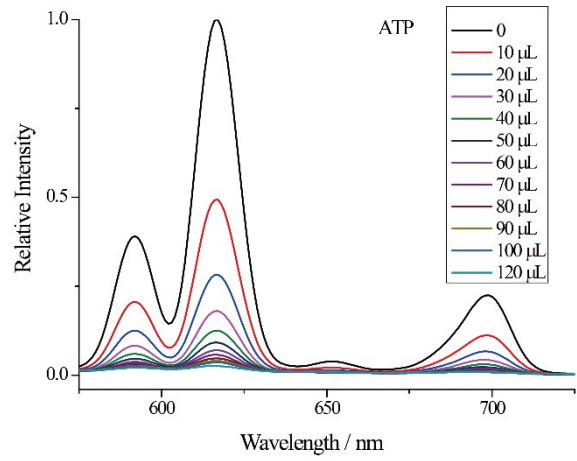
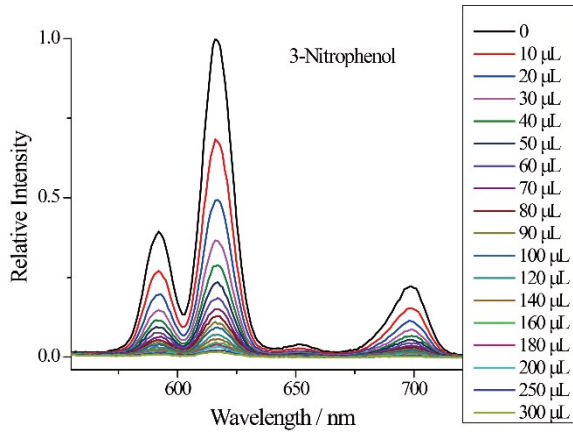


Fig. S10 Fluorescence spectra of compound 1 (ethanol suspension, 1.0 mL) before and after added different anions (excited at 265 nm).



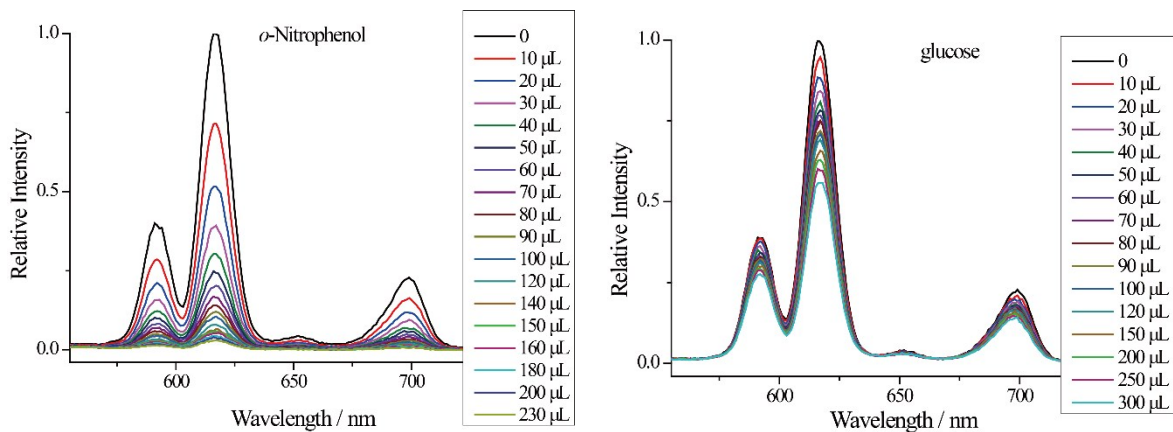
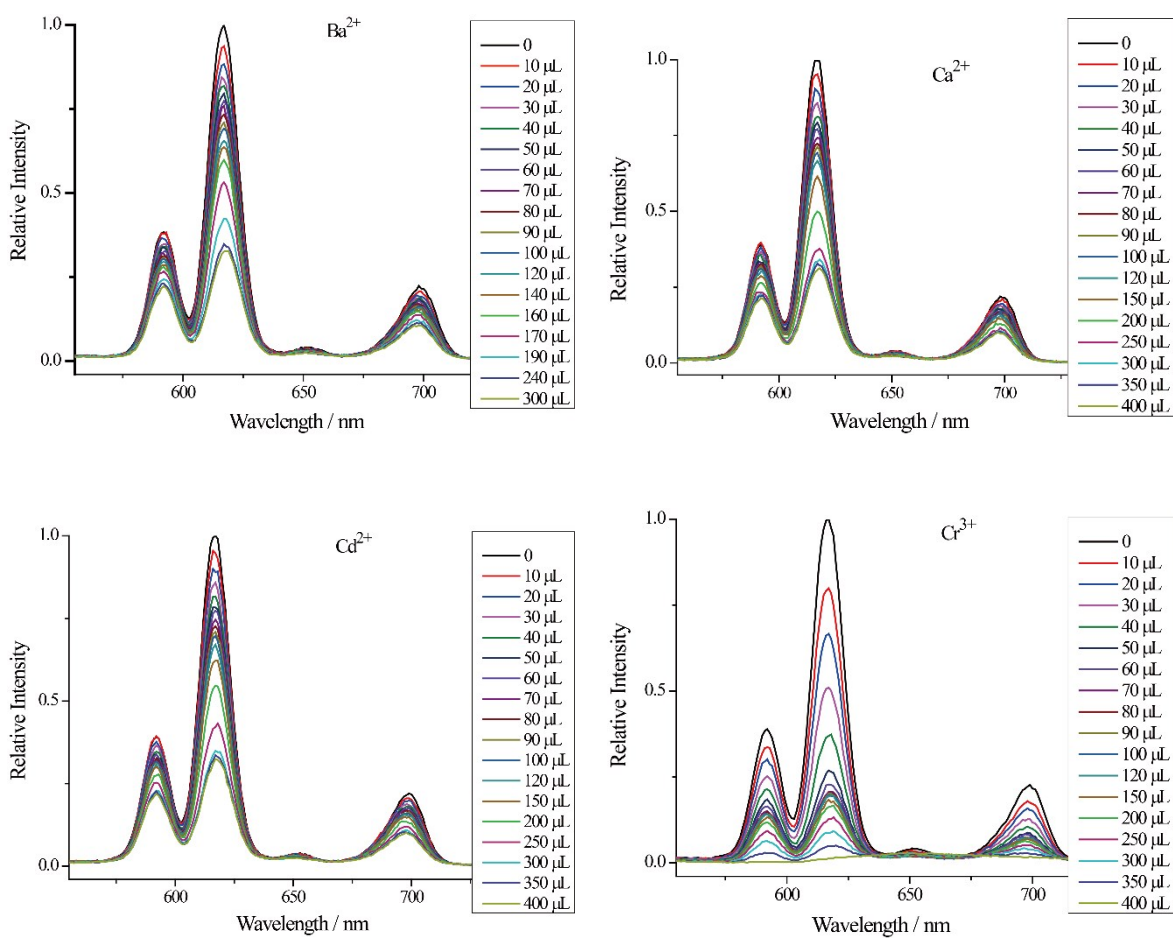


Fig. S11 Fluorescence spectra of compound **2** (ethanol suspension, 1.0 mL) before and after added various analytes (excited at 265 nm).



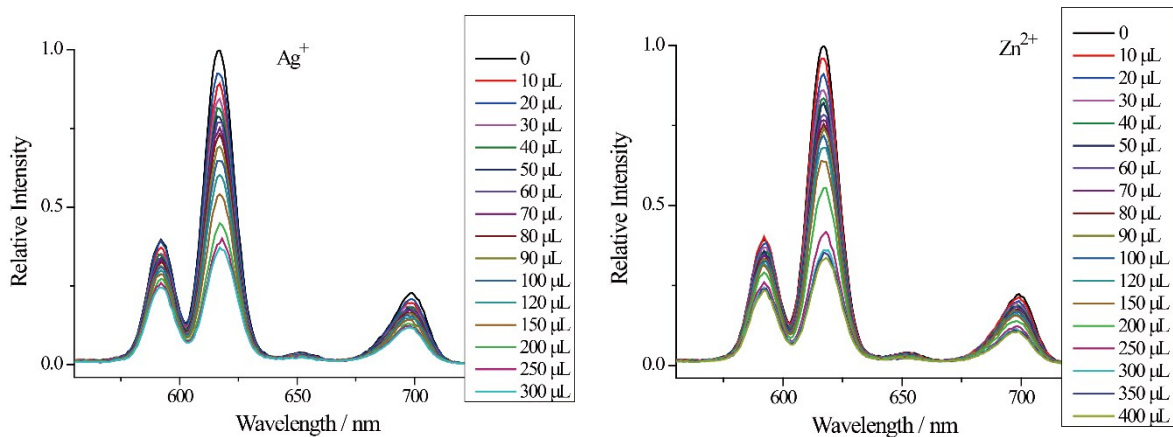
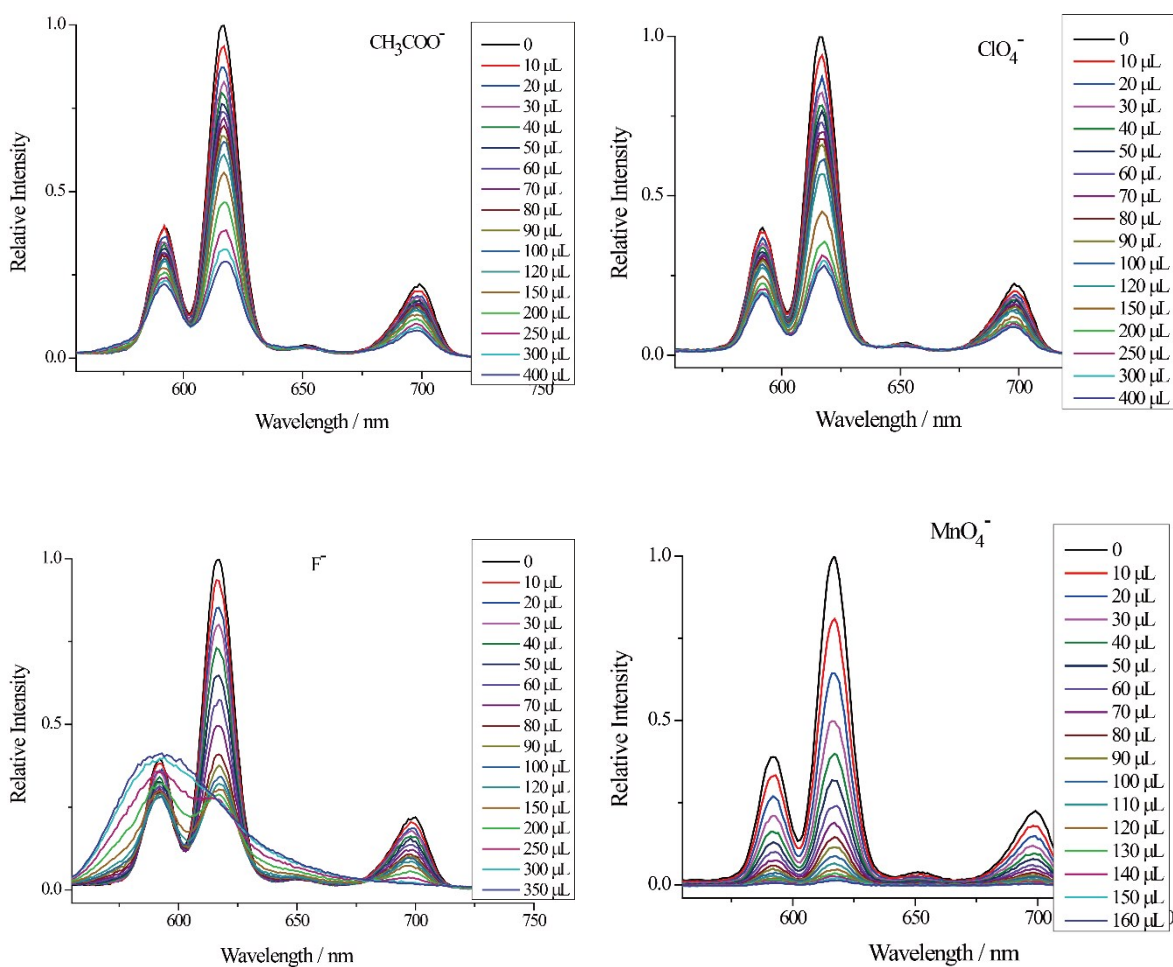
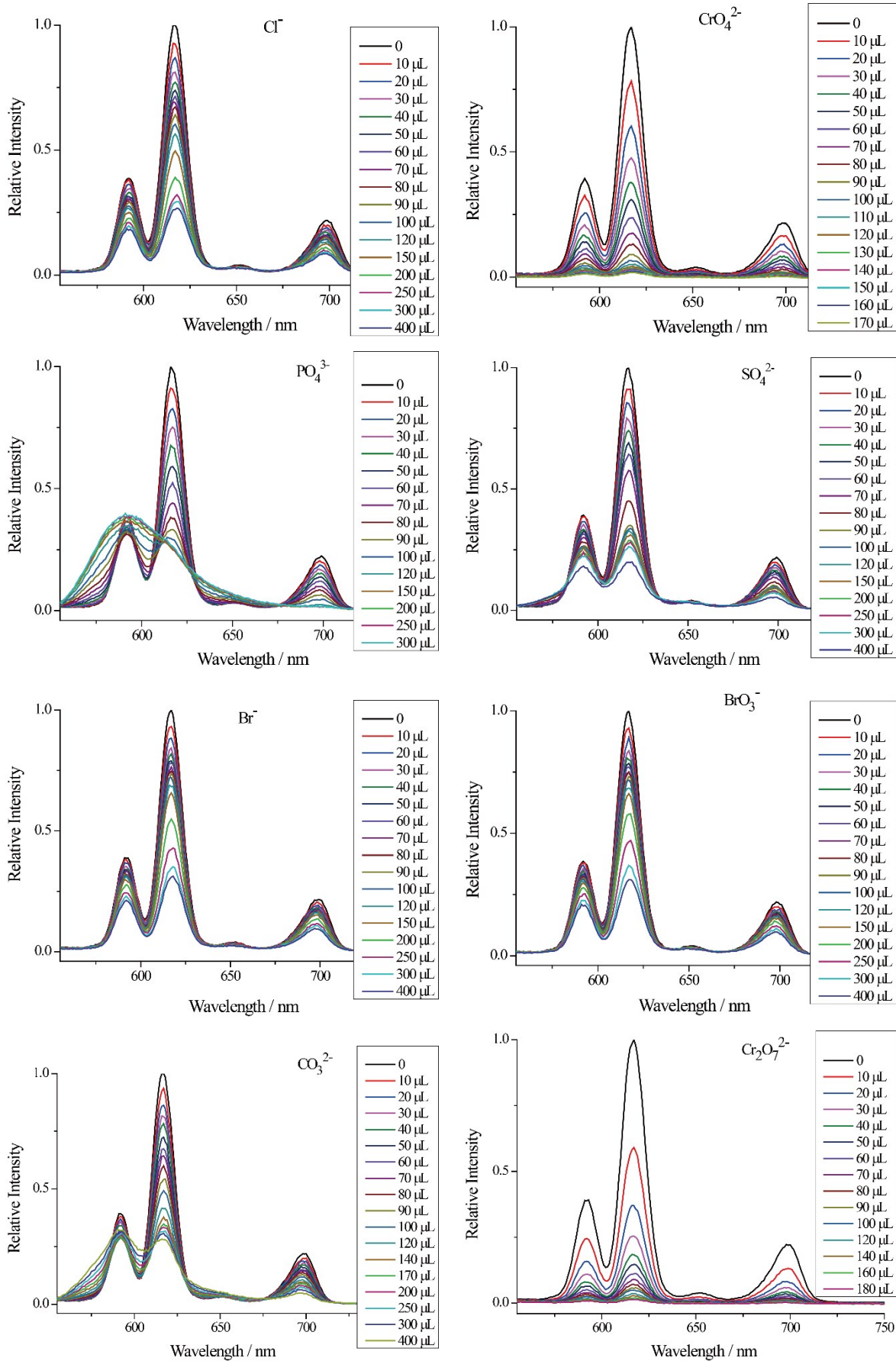


Fig. S12 Fluorescence spectra of compound **2** (ethanol suspension, 1.0 mL) before and after added different metal ions (excited at 265 nm).





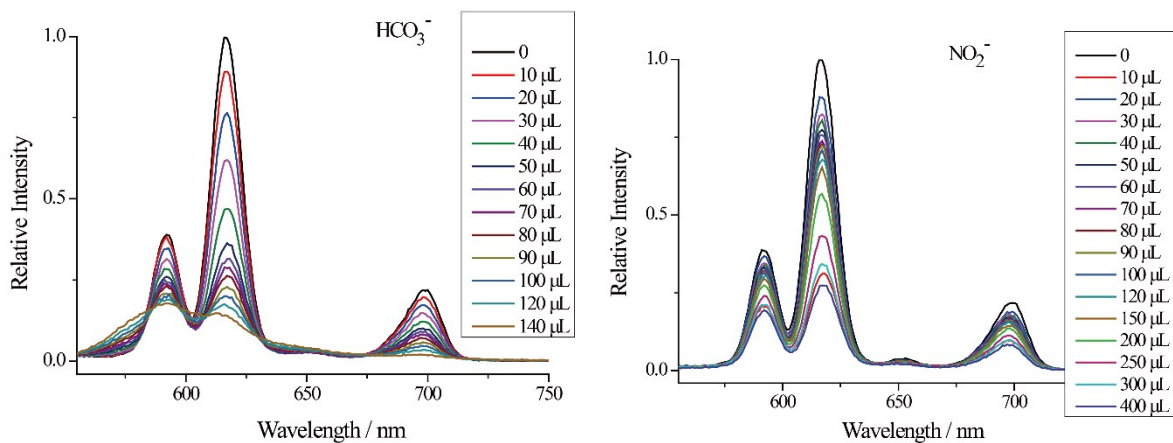


Fig. S13 Fluorescence spectra of compound **2** (ethanol suspension, 1.0 mL) before and after added different anions (excited at 265 nm).

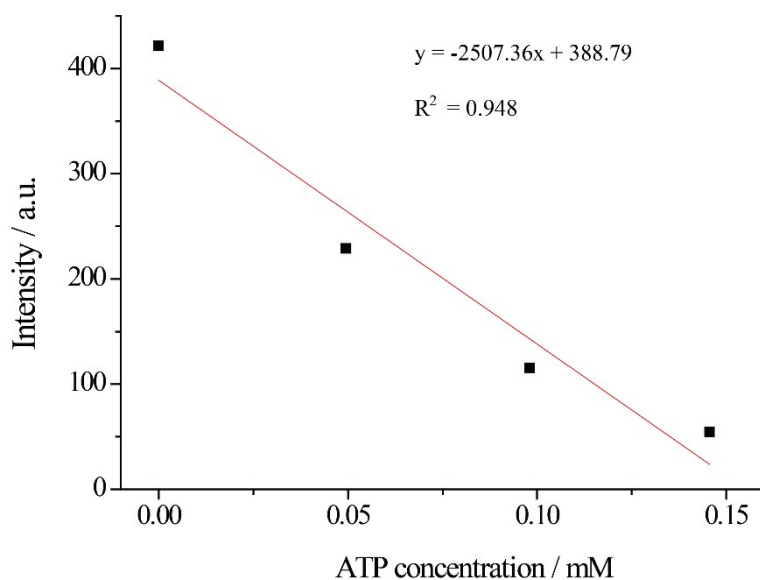


Fig. S14 The fitting curve of the emission intensity (617 nm) of compound **1** vs. ATP concentration.

Detection limit was determined according to the following definitions:

$$s_b = \sqrt{\frac{\sum_{i=1}^n (x_i - \bar{x})^2}{n-1}}$$

$$S = \frac{\Delta I}{\Delta c}$$

$$DL = \frac{3s_b}{S}$$

S is the slope of the calibration curve; S_b is the standard deviation for replicating detections of blank solutions.^[1]

$$S = 2.51 \times 10^6 \text{ M}^{-1}$$

$$S_b = 0.41 \text{ (n = 11)}$$

$$DL = 3S_b / S = 0.490 \times 10^{-6} \text{ M} = 0.490 \text{ } \mu\text{M} \text{ (for compound 1 detecting ATP)}$$

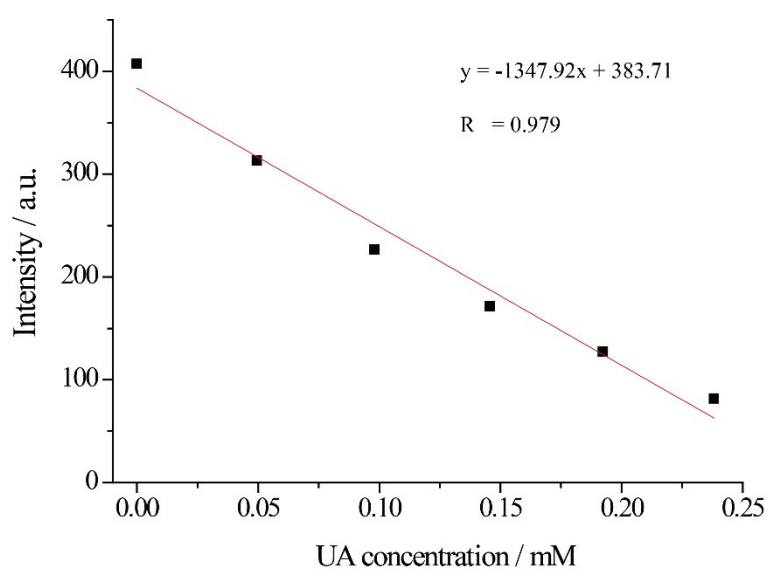


Fig. S15 The fitting curve of the emission intensity (617 nm) of compound **2** vs. UA concentration.

$$S = 1.347 \times 10^6 \text{ M}^{-1}$$

$$S_b = 0.27 \text{ (n = 11)}$$

$$DL = 3S_b / S = 0.601 \times 10^{-6} \text{ M} = 0.601 \text{ } \mu\text{M} \text{ (for compound 2 detecting UA)}$$

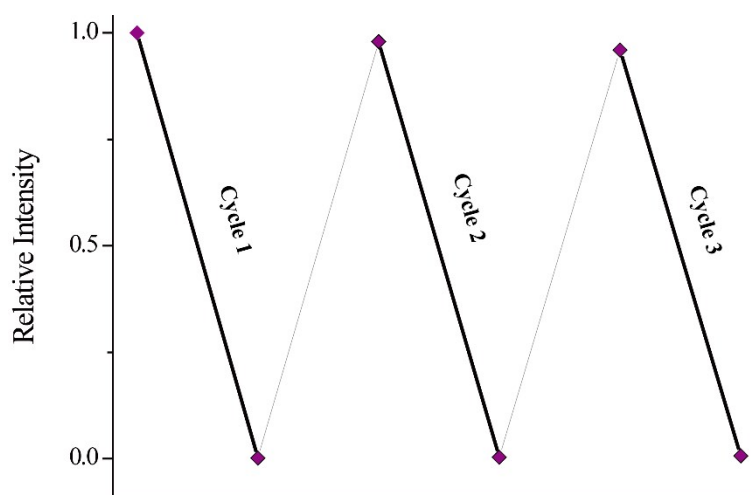


Fig. S16 Reproducibility of luminescence intensity (617 nm) of crystal powder compound **1** up to three cycles, adding ATP (100 μ L).

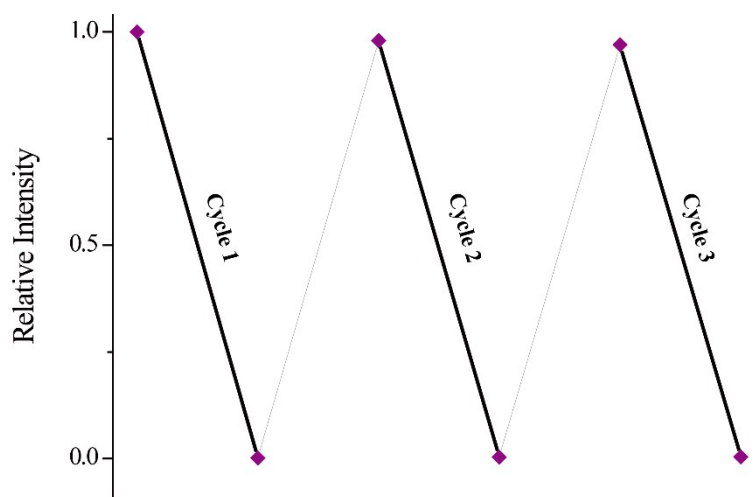


Fig. S17 Reproducibility of luminescence intensity (617 nm) of crystal powder compound **2** up to three cycles, adding UA(100 μ L).

Table S1 Selected bond lengths (Å) and angles (°) for compound **1**.

Eu(1)-O(3)	2.388(2)	O(3)-Eu(1)-O(5)	77.86(9)
Eu(1)-O(5)	2.396(2)	O(3)-Eu(1)-O(8)	115.72(8)
Eu(1)-O(8)	2.426(3)	O(5)-Eu(1)-O(8)	81.60(10)
Eu(1)-O(7)	2.432(2)	O(3)-Eu(1)-O(7)	74.88(8)
Eu(1)-O(4)	2.442(3)	O(8)-Eu(1)-O(7)	84.88(10)
Eu(1)-O(2)	2.487(3)	O(5)-Eu(1)-O(4)	73.97(9)
Eu(1)-O(1)	2.501(2)	O(8)-Eu(1)-O(4)	76.59(9)
Eu(1)-O(6)	2.550(2)	O(7)-Eu(1)-O(2)	86.87(10)
		O(4)-Eu(1)-O(2)	83.82(11)
		O(3)-Eu(1)-O(1)	81.54(8)
		O(5)-Eu(1)-O(1)	74.81(9)

Table S2 Selected bond lengths (Å) and angles (°) for compound **2**.

Eu(1)-O(12)	2.3834(18)	O(12)-Eu(1)-O(8)	70.83(9)
Eu(1)-O(8)	2.402(3)	O(8)-Eu(1)-O(7)	73.44(9)
Eu(1)-O(7)	2.4249(16)	O(7)-Eu(1)-O(9)	69.53(7)
Eu(1)-O(9)	2.4305(19)	O(12)-Eu(1)-O(2)	75.47(6)
Eu(1)-O(2)	2.4500(18)	O(9)-Eu(1)-O(2)	74.87(6)
Eu(1)-O(5)	2.4896(17)	O(12)-Eu(1)-O(5)	76.98(6)
Eu(2)-O(13)	2.3154(19)	O(9)-Eu(1)-O(5)	78.16(7)
Eu(2)-O(11)#1	2.3571(16)	O(2)-Eu(1)-O(5)	68.15(6)
Eu(2)-O(5)	2.3632(16)	O(12)-Eu(1)-O(10)	75.31(7)
Eu(2)-O(3)	2.3961(18)	O(8)-Eu(1)-O(10)	79.52(12)
Eu(2)-O(1)	2.443(2)	O(7)-Eu(1)-O(10)	91.46(7)
Eu(2)-O(4)	2.450(2)	O(2)-Eu(1)-O(10)	85.66(8)
		O(8)-Eu(1)-O(6)	76.58(12)
		O(7)-Eu(1)-O(6)	76.80(6)
		O(9)-Eu(1)-O(6)	79.34(9)

Symmetry transformations used to generate equivalent atoms: #1 $x, -y+1/2, z+1/2$

Table S3 Crystal data and structure refinement for **1** and **2**.

	1	2
Empirical formula	C ₁₈ H ₂₈ Eu ₂ O ₁₆	C ₃₀ H ₃₀ Eu ₂ O ₁₅
Formula weight	804.33	934.48
Crystal color	Yellow	Yellow
Crystal size (mm)	0.20 x 0.18 x 0.15	0.18 x 0.15 x 0.12
Crystal system	Triclinic	Monoclinic
space group	<i>P</i> $\bar{1}$	<i>P</i> 2 ₁ / <i>c</i>
a (Å)	7.909(2)	21.9083(13)
b (Å)	8.285(3)	10.1368(6)
c (Å)	10.444(3)	14.0410(8)
α (deg)	72.666(4)	0
β (deg)	74.008(4)	91.5660(10)
γ (deg)	78.581(4)	0
Volume (Å ³)	622.9(3)	3117.1(3)
Z	1	4
d _{calcd} (g/cm ³)	2.117	1.987
μ (mm ⁻¹)	5.063	4.062
F (000)	380	1816
λ (Å)	0.71073	0.71073
Temperature	293(2) K	293(2) K
θ range (deg)	2.10 to 27.00	0.93 to 27.17
h, k, l range	-10 ≤ h ≤ 9 -10 ≤ h ≤ 8 -13 ≤ h ≤ 10	-27 ≤ h ≤ 27 -8 ≤ h ≤ 12 -17 ≤ h ≤ 17
Reflections collected / unique	3624 / 2625 [R(int) = 0.0106]	18097 / 6816 [R(int) = 0.0364]
Completeness to θ	95.9 % (θ = 27.00)	98.7 % (θ = 27.17)
Data / restraints / parameters	2625 / 0 / 199	6816 / 0 / 537
Goodness-of-fit on F ²	1.044	1.126
Final R indices [I > 2σ(I)] ^a	R1 = 0.0194 wR2 = 0.0541	R1 = 0.0182 wR2 = 0.0452
R indices (all data)	R1 = 0.0195 wR2 = 0.0542	R1 = 0.0204 wR2 = 0.0461
Largest diff. Peak and hole (e ⁻ ·Å ⁻³)	0.955 and -1.124	0.501 and -0.590

References

- [1] Xu, H.; Gao, J.; Qian, X.; Wang, J.; He, H.; Cui, Y.; Yang, Y.; Wang, Z.; Qian, G. Metal–organic framework nanosheets for fast response and highly sensitive luminescent sensing of Fe^{3+} . *J. Mater. Chem. A*, 2016, **4**, 10900–10905.